Title: Uranium distribution as a proxy for basin scale fluid flow in distributive fluvial systems

Amanda Owen[1], A. J. Hartley[1], G. S. Weissmann[2], G. J. Nichols[3]

Corresponding authors email: a.owen@abdn.ac.uk

[1] Department of Geology & Petroleum Geology, University of Aberdeen, Aberdeen, AB24 3UE, U.K.

[2] University of New Mexico, Department of Earth and Planetary Sciences, MSC03 2040, Albuquerque, NM 87131-0001, U.S.A.

[3] Now at Nautilus Ltd., Ashfields Farm, Priors Court Road, Hermitage, Berkshire, RG18 9XY, U.K.

Abstract

We infer system scale fluid flow in the Late Jurassic Salt Wash fluvial succession (SW USA) by plotting uranium deposit distribution against sedimentological data, using uranium distribution as a proxy for subsurface fluid flow. More than 90% of Uranium deposits in the Salt Wash occur where sandstone comprises 40-55% and sand-rich channel-belts form 20-50% of the succession, which coincides with changes in channel-belt connectivity and gross-scale architecture. The paucity of uranium below these cut-off values, suggests fluid flow is related directly to predictable downstream fining and facies variations in distributive fluvial systems.

Key words: Connectivity, permeability, distributive fluvial systems, Salt Wash Member, Uranium.

Supplementary material [A summary table of location data, key trends and the amalgamation ratio methodology] is available at www.geolsoc.org.uk/SUP00000.

(1) Introduction

Fluvial deposits form globally important aquifers (e.g. Fitts, 2013) and oil and gas reservoirs (Keogh *et al*. 2007), as well as hosting mineral deposits such as uranium (e.g. Turner-Peterson, 1986), and exotic copper (e.g. Maiden *et al*. 1984). Exploitation of these resources requires understanding of regional fluid flow pathways within fluvial successions. Due to the typically limited availability of subsurface data, controls on regional fluid flow cannot necessarily be determined directly. To determine subsurface fluid flow pathways, an understanding of facies distribution is crucial as this controls sandstone connectivity, permeability and porosity (Renard, and Allard, 2013).

(1) Objectives and Methodology

We aim to document the relationship between uranium mineralisation, facies distribution and fluvial architecture in the Upper Jurassic Salt Wash distributive fluvial system (DFS), SW USA. We use the distribution of mineralisation as a proxy to assess controls on basin scale porosity and permeability distribution. These observations have important implications for understanding controls on subsurface fluid flow and will impact the exploration for and exploitation of aquifers, hydrocarbon reservoirs and sandstone-hosted strata-bound mineral deposits.

Uranium mineralisation in sandstone hosted deposits is considered to have been controlled by subsurface fluid flow and is closely related to sandstone body connectivity, porosity and permeability (Sanford, 1982; 1992). Uranium enriched fluids migrate through porous and permeable sandstone strata until precipitation occurs at an interface between oxidised and reduced rocks where two chemically different fluids meet (Abzalov, 2012). Massive sandstone bodies are considered to be effective flow conduits, and therefore possess good reservoir qualities, with mineralisation mainly limited to areas where permeable and impermeable strata interfinger (Gabelman, 1971; Abzalov, 2012).

Uranium distribution in the Salt Wash DFS (distributive fluvial system) provides a proxy for understanding subsurface fluid flow in an outcrop example at a basin-scale. The extensive exposure (100,000 km^2 Fig. 1) and trends in alluvial architecture (Owen *et al*. 2015b) provide a well constrained framework in which to conduct such a study. We integrate facies distribution, alluvial architecture and uranium deposit distribution to assess controls on uranium mineralisation. Uranium deposit distribution (Fischer, 1968) is plotted against sandstone and channel-belt percentage (Owen *et al*. 2015b) and compared to variations in fluvial architecture from field observations. An amalgamation ratio (A/R) (Zhang *et al*. 2013) is calculated to quantify and compare the degree of connectivity present at each location (see supplementary material).

(1) The Salt Wash DFS

The Salt Wash Member of the Late Jurassic Morrison Formation was deposited in a foreland basin (Decelles, 2004) as a DFS (for details of key DFS trends see Weissmann *et al*. (2013) and Owen *et al.* (2015b)). The apex of the Salt Wash system is predicted to be located in present day NW Arizona (Fig. 1A)(Owen *et al.* 2015a). The Salt Wash DFS is composed lithostratigraphically of relatively proximal facies (Salt Wash Member) that prograded into the basin over the distal facies (Tidwell Member), which underlie the Brushy Basin Member, completing the Morrison Formation. (e.g. Owen et al. 2015c). Overall the system shows typical characteristics of DFS deposits such as a downstream decrease in sandstone percentage (70% to 8%), channel presence (67% to 0%) and channel thickness (15 m to 3.8 m to the last measurable channel) with a concomitant increase in floodplain (38% to 94%) and lacustrine facies (0.1% to 7%) from proximal to distal (Owen et al. 2015a, b, c). A downstream change in deposit architecture is also evident. Proximal areas are dominated by amalgamated channel-belt complexes, which become increasingly separated by floodplain deposits downstream, and then pass into floodplain fines with sparse isolated channels (Owen *et al*. 2015b, c).

(1) Uranium distribution

Uranium in the Salt Wash DFS is largely considered to be of the tabular type but roll type deposits are also recognised (Dahlkamp, 2010). A description of the ore mineralogy can be found in Thamm *et al.* (1981). Two modes of ore formation are suggested (Fig. 1B): 1) the lacustrine-humate model (e.g. Peterson and Turner-Peterson, 1980) and 2) The brine interface model (e.g. Sanford, 1982; 1992). For both models it is clear that understanding controls on subsurface groundwater movement within the Salt Wash is key.

The relationship between known uranium deposit distribution and sandstone percentage is shown in Figure 2, with 92% (108/117) of uranium localities restricted to the 40-55% sandstone contour line with little or no uranium present below 40%. A broader relationship is present when uranium distribution is plotted onto channel-belt percentage maps with 90% (105/117) of uranium localities falling between the 20-50% channel-belt percentage contour lines (Fig. 2B, D).

From the 40-55% sandstone percentage and 20-50% channel-belt percentage zones a change in architecture is observed (Fig. 3). The gross-scale architecture at Atkinson Creek is typical of medial DFS facies (Fig. 3A), where channel-belt deposits are separated by laterally extensive floodplain deposits. Channel-belt deposits comprise 27.8% of the successions and average 4.5 m in thickness (maximum 8 m), and are up to 1.3 km in width (Owen *et al.* 2015b). Storey thickness within the channel-belts range from 0.7 to 5.3 m (Owen *et al*. 2015b). Using methods of Zhang et al. (2013), an A/R of 12% was calculated for Atkinson Creek, suggesting that there is limited but potentially important connectivity between channel-belt packages.

Further down system, a distinctive change in architecture associated with increased floodplain fines is observed at Little Park (Figs.1A, 3B). Amalgamated channel-belt deposits comprise 16.3% of the succession, and are on average 3.8 m thick and 800 m wide. An A/R ratio of 0% was calculated indicating that effective connectivity has been lost at this point in the system.

(1) Discussion

A clear relationship is present between uranium distribution, sandstone percentage, channel-belt percentage (Fig. 2) and fluvial architecture in the Salt Wash system (Fig. 3), indicating a sedimentological (i.e. facies) control on the distribution of uranium. We postulate that uranium distribution is related to down (depositional) dip variations in porosity and permeability, controlled by facies distribution.

Gabelman (1971) noted that areas of high permeability are not the most effective sites for uranium precipitation, as internal porosity and permeability barriers are required for concentration of uranium enriched fluids. Fluid barriers also need to occur in conjunction with the reducing conditions necessary for uranium mineralization. The lack of uranium in the proximal part of the Salt Wash DFS (Fig. 2) is in-part considered to be related to the high connectivity of channel-belts (see Table S2, supplementary material), due to repeated avulsions, channel occupation and reworking (Weissmann *et al*. 2013; Owen et al. 2015 c). An exception to this occurs in the Henry Mountains district (Fig. 2), where <6% of uranium sites occur due to local variations in subsidence that deflected regional flow (Sanford, 1992). Downstream, avulsions occur over a larger area and together with reduced sedimentation rates and channel bifurcation results in separation of the channel-belt sandstones by floodplain deposits (baffles) reducing vertical and lateral channel-belt connectivity (Fig 3). A lack of uranium NE of Atkinson Creek suggests channel-belt connectivity, and therefore large-scale system scale fluid flow connectivity, dissipates close to the 40 – 45% sandstone contour (Fig. 2A). This coincides with a change in regional scale architecture and a facies transition from medial to distal DFS deposits resulting in compartmentalization of fluid flow in sandstone bodies and precipitation from uranium-rich fluids (Fig 1B).

Once fluid flow is compartmentalised into discrete channel-belts, internal heterogeneities will play a key role in baffling fluid flow. Meander-belt deposits within channel-belt complexes are reported to be key sites for mineralisation in the Salt Wash (Stokes, 1954; Ethridge *et al*. 1980). Sanford (1992) relates uranium distribution to a combination of a regional change in sandstone: mudstone ratio, a change from low to high sinuosity channels, and change in total thickness. We concur that a large scale change in sandstone percentage plays a crucial control (Fig 2A), and here provide quantification of the precise location. However, we relate this to system scale changes in fluid flow, due to channel-belt connectivity and architectural changes across a DFS rather than changes in sinuosity. Hartley *et al.* (2015) show the preservation of an amalgamated meander belt, up-dip of the uranium belt, suggesting sinuous features are ubiquitous across the system. Trends observed in the Salt Wash are also apparent in the Westwater Canyon Member of the Morrison Formation, which is also interpreted to be a DFS (Turner-Peterson, 1986) where all the major uranium occurrences are located in mid-fan facies (Kyser and Cuney, 2009).

Larue and Hovadik (2006) provided a theoretical model in which reservoir sandstone body connectivity is considered to be good (> 90%) when the sandstone percentage is > 30%. It is important that the geometry and form of the deposits is also considered, which the amalgamation ratio helps us achieve. We therefore suggest a higher cut off of 40% should be used as our data from a rock record example shows that effective connectivity between channel-belt deposits starts to diminish at 55% and that by 40% an A/R of 12% present. However, internal permeability within the channel-belt must be considered and further statistical analysis is needed to test this robustly.

Understanding system scale porosity and permeability variations is crucial when exploring and understanding migration pathways of key resources. Although other post-depositional factors such as cementation or compaction (Hazeldine *et al*. 2000) need to be considered, we provide an understanding of primary basin scale trends and controls. Our unique dataset relating uranium distribution to sandstone percentage allows context to be given to the uranium deposits, improving understanding of fluid flow in DFS deposits. Due to its quantified nature, results from this study can be related directly to subsurface datasets aiding exploration and recovery of key resources.

(1) Conclusions

We suggest that Uranium distribution within the Salt wash DFS can be used as a proxy for understanding basin scale porosity and permeability variations. Clear relationships are present between uranium mineralisation and sandstone and channel-belt percentage maps with 92% of mineralisation concentrated at the 40-55% sandstone, and 90% in the 20-50% channel-belt percentage contours respectively. The amalgamation ratio and field evidence indicates that this is a critical point at which effective connectivity is lost, as a drop from 38% in the proximal region to 12% at Atkinson Creek to 0% at Little Park is observed, allowing internal porosity and permeability variations to concentrate uranium-bearing fluids, with precipitation occurring when reducing conditions are met. We relate changes in channel-belt connectivity to predictable downstream facies variations in the DFS model, providing a system scale model of subsurface fluid flow in a DFS. Results will aid prediction of uranium occurrence in similar settings, and the addition of statistics such as sandstone and channel-belt percentage makes this study directly applicable to subsurface successions.

Acknowledgements

This work was supported by the Fluvial Systems Research Group sponsors BG Group, BP, Chevron, ConocoPhilips, and Total. We thank reviews from Martin Stokes, an anonymous reviewer and Editor Stuart Jones.

References

Abzalov, M.Z. 2012. Sandstone-hosted uranium deposits amenable for exploitation by in situ leaching technologies. *Applied Earth Science*, **52**, 55–64.

Dahlkamp, F.J. 2010. Colorado Plateau, *In* Dahlkamp, F.J. (ed.) *Uranium deposits of the world USA and Latin America.* Springer-Verlag Heidelberg, 9–148.

Decelles, P.G. 2004. Late Jurassic to Eocene evolution of the Cordilleran thrust belt and foreland basin system, western U.S.A. *American Journal of Science,* **304**, 105–168.

Ethridge, F.G., Ortiz, N. V, Sunada, D.K., & Tyler, N. 1980. Laboratory, Field, and Computer Flow Study of the Origin of Colorado Plateau Type Uranium Deposits. *Second Interim Report: U.S. Geological Survey Open-File Report 80-805*.

Fischer, R. P. 1968. The uranium and vanadium deposits of the Colorado Plateau region. *In* Ridge, J. (ed.) *Ore deposits of the United States 1933-1967 (Graton Sales Volume)*. American Institute of Mining, Metallurgical, and Petroleum Engineers, New York, 735-746.

Fitts, C.R. 2013. Groundwater Science, 2nd edition Waltham, MA, Academic Press, 672p.

Gabelman, J.W. 1971. Sedimentology and uranium prospecting. *Sedimentary Geology*, **6**, 145–186.

Hartley, A.J., Owen, A., Swan, A., Weissmann, G.S., Holzweber, B.I., Howell, J., Nichols, G.J., Scuderi, L.A. 2015. Recognition and importance of amalgamated sandy meander belts in the continental rock record. *Geology*, **43**, 679-682.

Haszeldine, R. S., Macaulay, C. I., Marchand, A., Wilkinson, M., Graham, C. M., Cavanagh, A., Fallick, A. E., & Couples, G. D. 2000. Sandstone cementation and fluids in hydrocarbon basins. *Journal of Geochemical Exploration*, **69-70**, 195-200.

Keogh, K.J., Martinius, A.W., & Osland, R. 2007. The development of fluvial stochastic modelling in the Norwegian oil industry: A historical review, subsurface implementation and future directions. *Sedimentary Geology*, **202**, 249–268.

Kyser, K., & Cuney, M. 2009. Sandstone-hosted uranium deposits. *In* Cuney, M. and Kyser, K. (ed.) *Mineralogical Association of Canada Short Course Series Volume 39, Recent and not-so-recent developments in uranium deposits and implications for exploration*. Mineraological Association of Canada and Society for Geology Applied to Mineral Deposits, Québec, 221–240.

Larue, D.K., & Hovadik, J. 2006. Connectivity of channelized reservoirs: A modelling approach. *Petroleum Geoscience*, **12**, 291–308.

Maiden, K.J., Innes, A.H., King, M.J., Master, S., & Pettitt, I. 1984 Regional controls on the localisation of stratabound copper deposits: Proterozoic examples from Southern Africa and South Australia *Precambrian Research*, **25**, 99–118.

Owen, A., Jupp, P.E., Nichols, G.J., Hartley, A.J., Weissmann, G.S., & Sadykova, D. 2015a. Statistical estimation of the position of an apex: Application to the geological record. *Journal of Sedimentary Research*, **85**, 142–152.

Owen, A., Nichols, G.J., Hartley, A.J., Weissmann, G.S., & Scuderi, L.A. 2015b Quantification of a distributive fluvial system: The Salt Wash DFS of the Morrison Formation, SW USA. *Journal of Sedimentary Research,* ***84***, 544-561.

Owen, A., Nichols, G.J., Hartley, A.J., & Weissmann, G.S. 2015c Vertical trends within the prograding Salt Wash distributive fluvial system, SW United States. *Basin Research,* 1-17, DOI: 10.1111/bre.

Peterson, F., & Turner-Peterson, C.E. 1980. Lacustrine-humate model: Sedimentological and geochemical model for tabular sandstone uranium deposits in the Morrison Formation, Utah, and application to uranium exploration. *U.S. Geological Survey Open File Report 80-319*.

Renard, P, and Allard, D., 2013, Connectivity metrics for subsurface flow and transport: Advances in Water Resources, v. 51, p. 168-196.

Sanford, R.F. 1982. Preliminary model of regional Mesozoic groundwater flow and uranium deposition in the Colorado Plateau. *Geology*, 10, 348–352.

Sanford, R. F. 1992 A new model for tabular-type Uranium deposits *Economic Geology*, **87**, 2041–2055.

Stokes, W.L. 1954. Some stratigraphic, sedimentary and structural relations of Uranium deposits in the Salt Wash Sandstone. *United States atomic energy final report RME-3102*.

Thamm, J.K., Kovschak, A.A., & Adam, S.S. 1981. Geology and recognition criteria for sandstone uranium deposits of the Salt Wash type, Colorado Plateau province. *National uranium resource evaluation report JFBX-6(81)*.

Turner-Peterson, C.E. 1986. Fluvial sedimentology of a major Uranium-bearing sandstone - A study of the Westwater Canyon Member of the Morrison Formation, San Juan Basin, New Mexico. *In* Turner-Peterson, C.E., Santos, E.S., and Fishman, N.S. (eds.) *A basin analysis case* *study - The Morrison Formation, Grants Uranium Region, New Mexico: American Association of Petroleum Geologists, Studies in Geology No 22*, 47–76.

Weissmann, G.S., Hartley, A.J., Scuderi, L.A., Nichols, G.J., Davidson, S.K., Owen, A, Atchley, S.C., Bhattacharyya, P., Chakraborty, T., Ghosh, P., Nordt, L.C., Michel, L., & Tabor, N.J. 2013. Prograding distributive fluvial systems - geomorphic models and ancient examples. *In* Dreise, S. G., Nordt, L.C., and McCarthy, P.L., (eds.) *New Frontiers in Paleopedology and Terrestrial paleoclimatology SEPM, Special Publication 104*, 131–147.

Zhang, L. Manzocchi, T., Haughton, P.D.W. (2013) Impact of Sedimentological Hierarchy on Sandstone Connectivity in Deep-Water Lobes – and Object-Based Modelling Approach. 75th EAGE Conference & Exhibition, London, UK, 10-13 June 2013.

Figure captions

Figure 1.A: Paleogeographical map of the study area with broad paleocurrent direction (modified from Owen *et al*. 2015a). B: Schematic of the lacustrine humate (Peterson and Turner-Peterson, 1980) and the brine interface (Sanford, 1992) models. Modified from Sanford (1992). Note fluid migration through facies belts within the Salt Wash. Line of cross-section can be seen in A.

Figure 2.A: Uranium distribution plotted onto sandstone percentage maps (modified from Owen *et al*. 2015b). The majority of uranium falls between 55% and 40% sandstone. B: Uranium distribution plotted onto channel-belt percentage maps (modified from Owen *et al*. 2015b). The majority of uranium falls between 50%-20%. C: Uranium distribution plotted against distance downstream and sand percentage intervals (grouped into 10% intervals). D:

Uranium distribution plotted against distance downstream and channel belt percentage. Uranium distribution taken from Fischer (1968). Table S2 of supplementary material shows the contrasting architecture observed in the zone of uranium concentration in comparison to the proximal and distal zones.

Figure 3 A: Architectural panel of Atkinson Creek. B: Architectural panel of Little Park. Note the difference in architectural styles, A contains laterally extensive channel belt deposits that are separated by floodplain fines which do at times amalgamate, whereas B is dominated by floodplain fines with rare channel belt presence and connectivity. See Fig. 1A for location of panels.

Figure 1

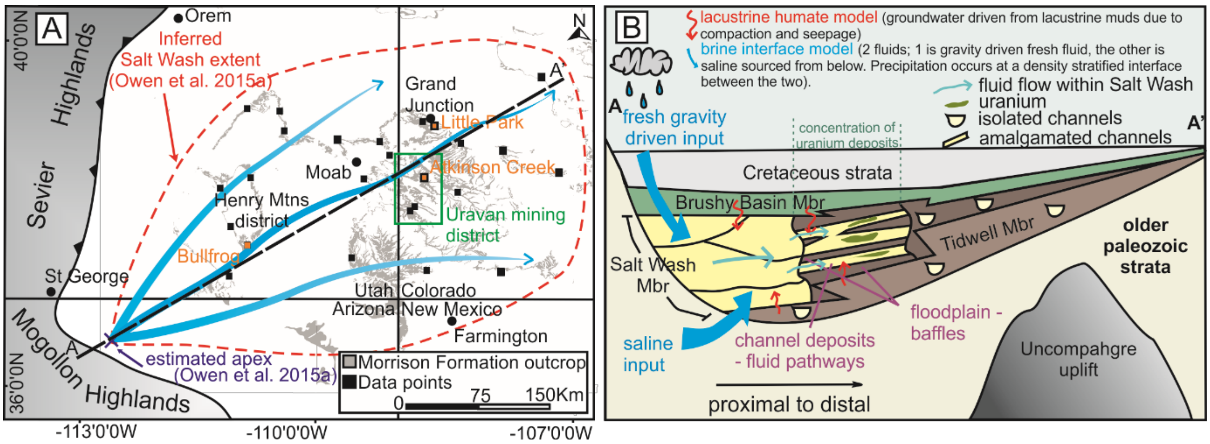

Figure 2

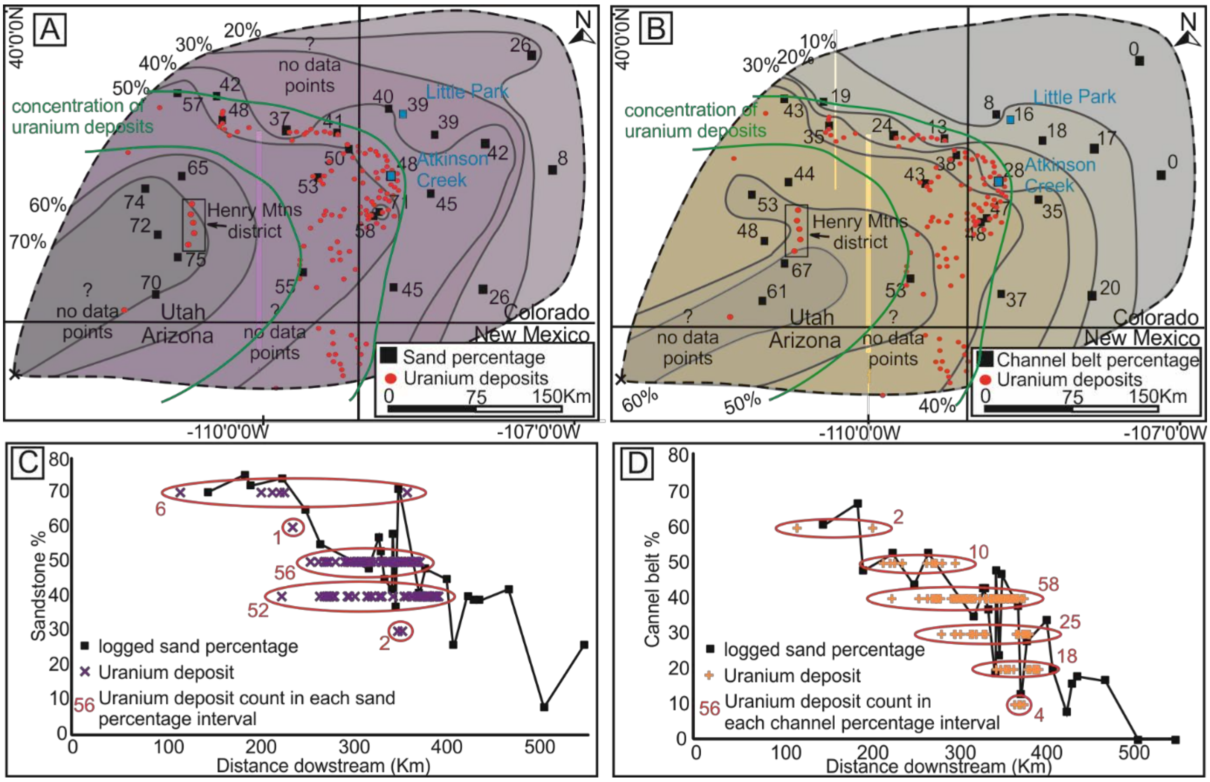

Figure 3

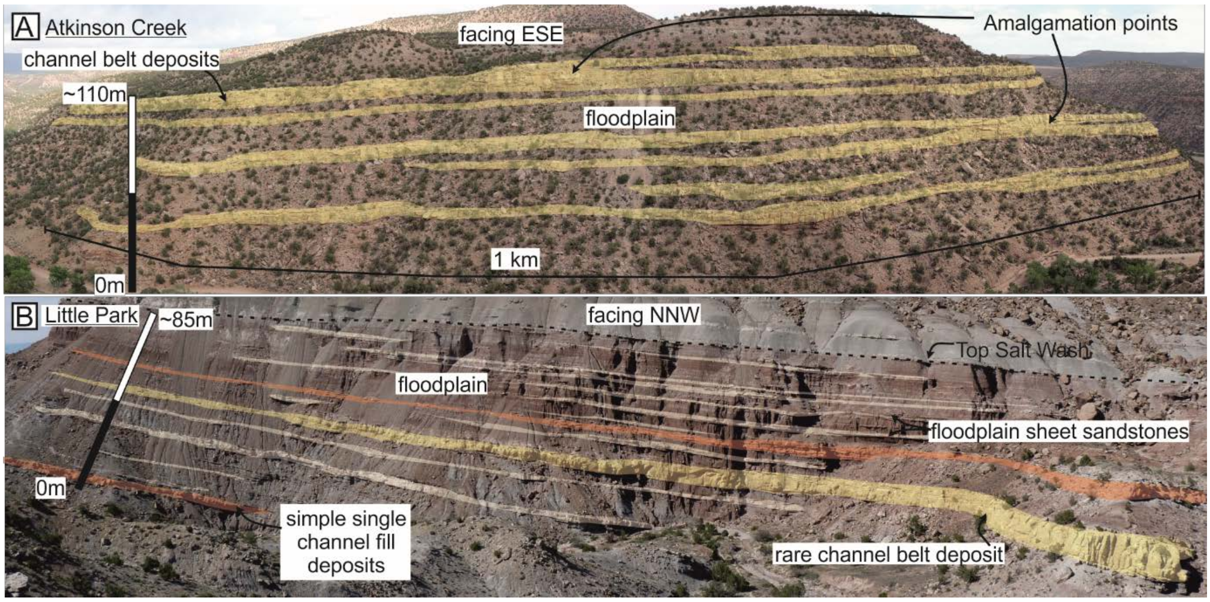

Supplimentary material 1 – amalgamation ratio

The amalgamation ratio has been calculated for each study site. The amalgamation ratio within this paper is defined as the fraction of channel-belt bases that are in contact (i.e. amalgamated) with lower channel-belts, modified from Zhang *et al*. (2013). For each channel base the total length of channel-on-channel contact (blue in Fig. S1.1) was divided by the total length of the channel base (red vertical line in Fig. S1.1). The sum of all channel-on-channel contacts within the panel were then divided by the sum of all channel base lengths, and then multiplied by 100 so that the amalgamation ratio within a panel could be expressed as a percentage. Table S1 shows the calculations for each site.

	Sandstone body	**Total Sandstone body length (m)**	**Channel-on-channel contact length (m)**	**Amalgamation ratio (%)** (length of channel-on-channel contact / Total channel belt length, X 100)
Proximal	1	375	139	37
	2	500	205	41
	3	500	340	68
	4	500	205	41
	5	500	50	10
	6	300	87	29
	7	475	38	8
	8	500	500	100
	9	500	0	0
	Whole panel	4150	1564	38
Medial	1	900	567	63
	2	900	0	0
	3	900	90	10
	4	900	0	0
	5	900	0	0
	6	300	0	0
	7	900	0	0
	Whole panel	5700	657	12
Distal	N/A. No amalgamation observed.			

Table S1. Table showing calculations for the amalgamation ratio for each site. Note that lengths are for the panels shown in Figure S1, not for the whole outcrop photo.

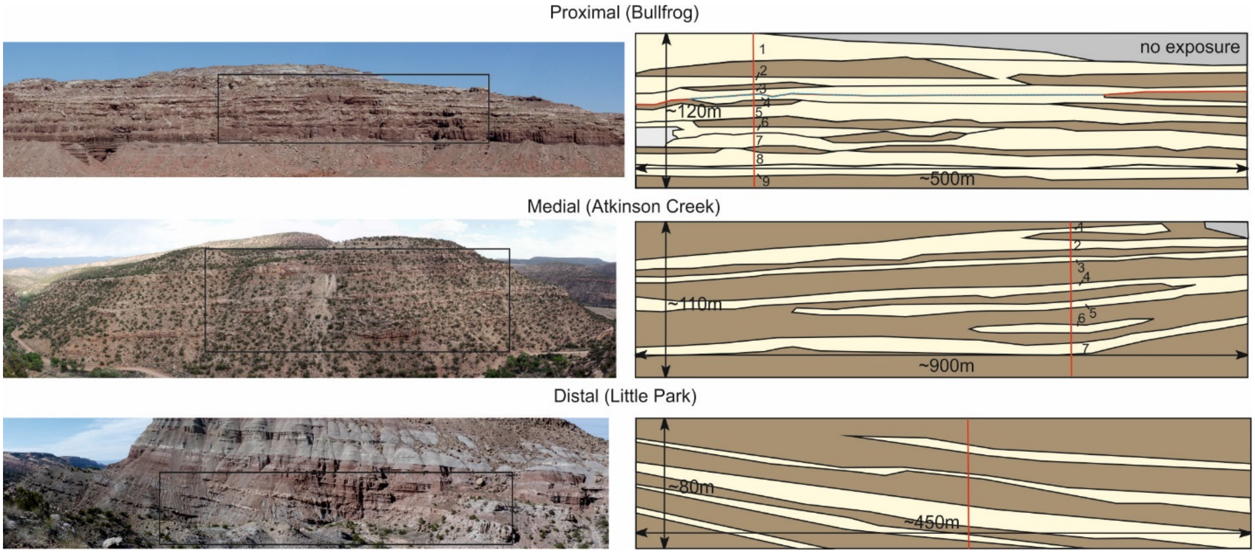

Figure S1.1. Panels for proximal, medial and distal locations on the Salt Wash DFS. See Figure 1A for location. Box on the photo panel indicates where the interpretation panel has been taken from. Red vertical line indicates where on the interpretation panel the number of sandbodies has been defined. See table S1 for statistics on each sandbody. Numbers define the sandbody number in Table S1. Colour on the interpreted panels: yellow = channel deposits, brown = floodplain, grey = no exposure.

Supplimentary material 2 – DFS characterisitcs

Channel belt %	Isolated channel %	Floodplain %	Max, average, min channel belt thickness (m)	Max channel belt width (km)	Amalgamat-ion ratio (%)	Facies architecture description	Representative archite (yellow = channel, brow
66.7	1.8	29.9	26 , 9.1, 1.8	> 5	38	Successions dominated by large scale amalgamated channel-belt deposits. Limited preservation of floodplain material, but when present it rarely extends the length of the outcrop.	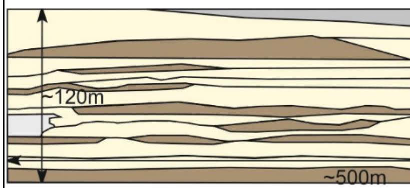
27.8	1.8	69.6	8, 4.5, 0.7	1.3	12	Succession contains channel-belt deposits that are seperated by distinctive floodplain deposits that do extend the length of the outcrop. Channel-belt deposits intermittently amalgamate.	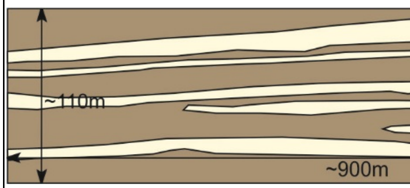
16.3	9.9	69.6	9.5, 3.8, 3.7	0.8	0	Channel-belt deposits are largely absent, and isolated channel deposits become more frequent. Little to no amalgamation of channel deposits.	

Table S2. Sandstone, channel belt, isolated channel and floodplain percentages taken from Owen *et al*. (2015b) for proximal, medial and distal locations. Channel belt amalgamation was calculated by dividing the length of amalgamation along a sandstone body by total length of the sandstone body and multiplying by 100 to gain a percentage. Note the change in architecture from proximal to medial. Uranium is found to be concentrated in the heterolithic medial zone where channel belt deposits are separated by floodplain fines.